ResearchGate

See discussions, stats, and author profiles for this publication at: https://www.researchgate.net/publication/326535821

Research on the Size Effect of Specific Cutting Energy Based on Numerical Simulation of Single Grit Scratching

Article *in* Journal of Manufacturing Science and Engineering · May 2018

DOI: 10.1115/1.4039916

CITATIONS
5

READS
132

4 authors, including:

Tao Zhang
National Huaqiao University
11 PUBLICATIONS **75** CITATIONS

SEE PROFILE

Feng Jiang
National Huaqiao University
91 PUBLICATIONS **681** CITATIONS

SEE PROFILE

Some of the authors of this publication are also working on these related projects:

Project flashzy1980@163.com View project

Project Micro/nano fabrication of high-performance polymeric films View project

All content following this page was uploaded by Tao Zhang on 04 September 2018.

The user has requested enhancement of the downloaded file.

Tao Zhang
Institute of Manufacturing Engineering,
Huaqiao University,
Xiamen 361021, China;
Engineering Research Center for Brittle
Material Intelligent Manufacturing Technology,
Fujian Province,
Xiamen 361021, China

Feng Jiang[1]
Institute of Manufacturing Engineering,
Huaqiao University,
Xiamen 361021, China;
Engineering Research Center for Brittle
Material Intelligent Manufacturing Technology,
Fujian Province,
Xiamen 361021, China
e-mail: jiangfeng@hqu.edu.cn

Lan Yan
College of Mechanical
Engineering and Automation,
Huaqiao University,
Xiamen 361021, China;
Engineering Research Center for Brittle
Material Intelligent Manufacturing Technology,
Fujian Province,
Xiamen 361021, China

Xipeng Xu
Institute of Manufacturing Engineering,
Huaqiao University,
Xiamen 361021, China;
Engineering Research Center for Brittle
Material Intelligent Manufacturing Technology,
Fujian Province,
Xiamen 361021, China

Research on the Size Effect of Specific Cutting Energy Based on Numerical Simulation of Single Grit Scratching

A method of research on the size effect of the specific cutting energy based on the numerical simulation has been proposed. The theoretical model of the research on size effect of specific cutting energy using single grit scratching simulation has been presented. A series of single grit scratch simulations with different scratching depths have been carried out to acquire different material removal rates. Then, the specific cutting energy has been calculated based on the power consumed and the material removal rate. The relationship between the specific cutting energy and the material removal rate has been given which agrees well with that presented by Malkin. The simulation results have been analyzed further to explain the size effect of specific cutting energy.
[DOI: 10.1115/1.4039916]

Keywords: size effect, specific cutting energy, single grit scratching, numerical simulation

1 Introduction

The specific grinding energy is defined as the energy consumed per unit volume of material removal during grinding process. The phenomenon that specific grinding energy decreases with the increase of grinding depth or sectional area of the chip is called size effect. The size effect was first presented by Shaw [1], and then, Malkin validated the existence of the size effect [2]. Malkin presented that total grinding energy consists of cutting and sliding energy [3]. Even after subtracting the sliding energy, the size effect still exists [4–6]. The phenomenon that specific cutting energy increases with the decrease of material removal rate is called size effect of specific cutting energy.

The size effect during grinding process is composed of the size effect of the sliding energy and cutting energy. The sliding energy is caused by the wear flat on the tip of grit according to the description of Malkin, and the wear flat is difficult to avoid for high speed scratching. Therefore, the study of size effect of specific cutting energy is extremely difficult due to the companion of sliding energy. Most of the studies focused on the size effect as a whole [7]. There are several different explanations of the size effect. Shaw presented that the existence of size effect results from the metal internal defects [1]. Because the probability is small that small-volume metal contains dislocation, so the small nondeformed chip thickness corresponds to a higher flow stress. But it was found that the density of dislocation is large in the shear zone in metal cutting experiments [8]. It is obvious that this theory is not a good explanation for size effect. Pashley gave an explanation of size effect from the view of work hardening [9]. Rowe and Chen explained the size effect by the presentation of "sliced bread analogy" [10]. Size effect is a very complex phenomenon, and a previous research showed that specific energy during grinding process is related not only to grinding process parameters, but also to the mechanical properties of the workpiece material [11]. It is extremely different to study size effect of specific cutting energy by experiment due to the exist of wear flat in reality, and few literatures focused on the size effect of specific cutting energy during grinding process due to the extremely low realizability.

Grinding is a very complex process. It is a common method to abstract the complicated scientific problems to simple problems by academic analysis and experimental research. Therefore, the study of the grit–workpiece interaction through single grit scratching test is an important contribution to the explanation of the

[1]Corresponding author.

Manuscript received March 31, 2017; final manuscript received April 3, 2018; published online May 21, 2018. Assoc. Editor: Kai Cheng.

Copyright © 2018 by ASME

Downloaded From: http://manufacturingscience.asmedigitalcollection.asme.org/ on 08/28/2018 Terms of Use: http://www.asme.org/about-asme/terms-of-use

physical processes that occur during grinding. Single grit scratching test has been widely used to study the material removal mechanism [12,13]. Numerical simulation could reveal the phenomena that are difficult to investigate or unclear in the material removal mechanism and has been widely used in single grit scratching process [14–16].

In this study, a method of research on the size effect of the specific cutting energy based on the numerical simulation has been proposed. The theoretical model of the research on the size effect of specific cutting energy using single grit scratching simulation has been presented, and the specific cutting energy has been calculated based on the power consumed and the material removal rate. The relationship between the specific cutting energy and the material removal rate has been given. The conclusion has been got that the flow stress increases with the decrease of removal rate, which explains the relationship between specific cutting energy and material removal rate well. It is also found that the pile-up ratio decreases with the increase of scratching depth, which could explain the size effect of specific cutting energy from another perspective.

2 Theoretical Model

The removal of the metallic material is achieved by the formation of chips in the grinding process. However, most of the grinding energy is not consumed by the formation of chips but by wear flat of grit slides on the surface of workpiece, but the sliding process cannot remove material. The working condition of a single grit in grinding process is shown in Fig. 1. Malkin presented that the grinding forces and specific grinding energy consists of cutting and sliding. So the forces applied on the single grit and specific grinding energy can be expressed as [3]

$$F_t = F_{t,c} + F_{t,sl} \tag{1}$$

$$F_n = F_{n,c} + F_{n,sl} \tag{2}$$

$$u = u_c + u_{sl} \tag{3}$$

where F_n and F_t are the tangential and normal force applied on the single grit, respectively. $F_{t,c}$ and $F_{n,c}$ are the tangential and normal force for cutting, and $F_{t,cl}$ and $F_{n,cl}$ are those for sliding. The u is specific grinding energy; u_c and u_{sl} are specific cutting energy and specific sliding energy, respectively.

As shown in Fig. 1. There is a wear flat on the tip grit. For steel workpiece, the sliding forces are proportional to the area of the wear flat. So the forces applied on the single grit could also be expressed as [3]

$$F_t = F_{t,c} + \mu \bar{p} A_a \tag{4}$$

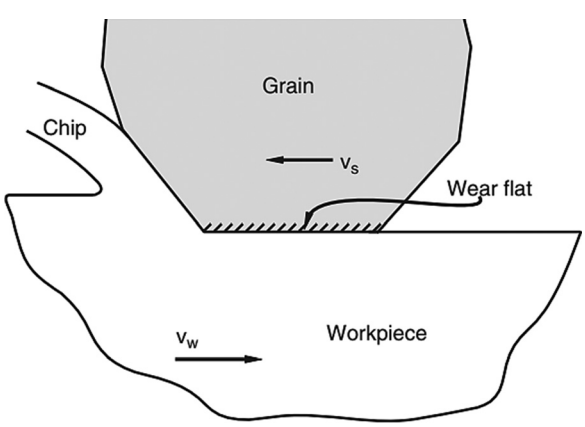

Fig. 1 The working condition of a single grit [3]

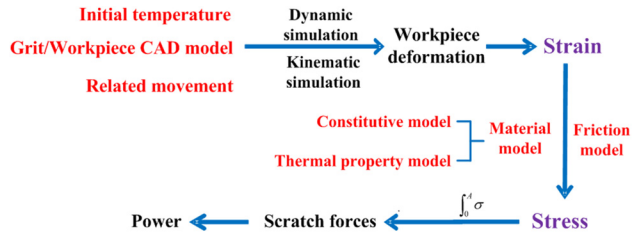

Fig. 2 The procedure of numerical calculation

$$F_n = F_{n,c} + \bar{p} A_a \tag{5}$$

where $\bar{p}$ is the average contact stress between grit and workpiece, and μ is the coefficient of friction. A_a is the area of wear flat.

In general, girt can be simplified as a cone with a spherical tip. When the tip of ideal grit is always no wear exists that is the area of wear flat is equal to zero, then the $F_{t,cl}$ and $F_{n,cl}$ and u_{sl} can be ignored, and Eqs. (1)–(3) can be simplified as following:

$$F_t = F_{t,c} \tag{6}$$

$$F_n = F_{n,c} \tag{7}$$

$$u = u_c \tag{8}$$

The research process of the relationship between the specific cutting energy and the material removal rate can be greatly

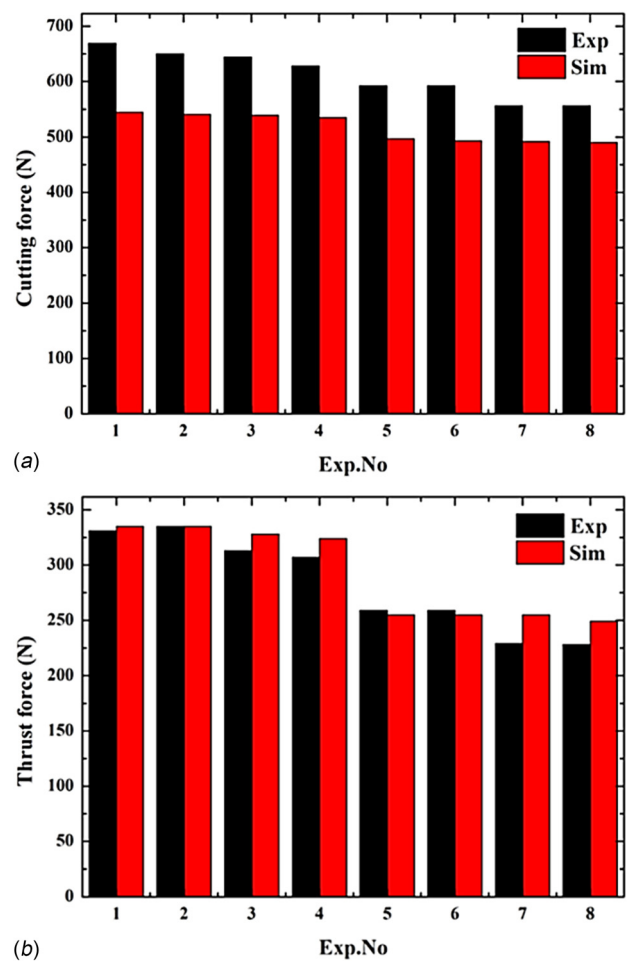

Fig. 3 Comparison of simulation and test results: (*a*) cutting force and (*b*) thrust force

Downloaded From: http://manufacturingscience.asmedigitalcollection.asme.org/ on 08/28/2018 Terms of Use: http://www.asme.org/about-asme/terms-of-use

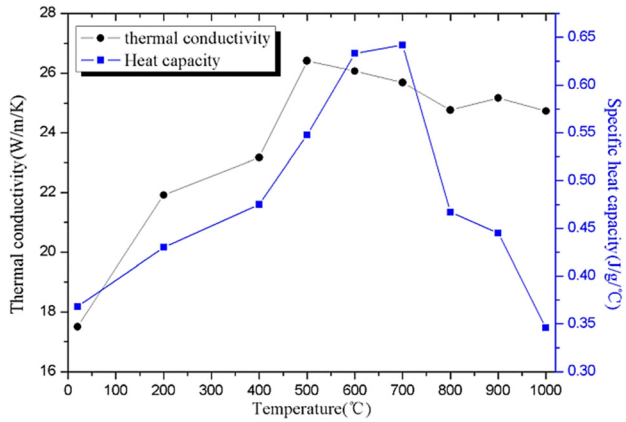

Fig. 4 The thermal conductivity and heat capacity Fe–Cr–Ni stainless steel

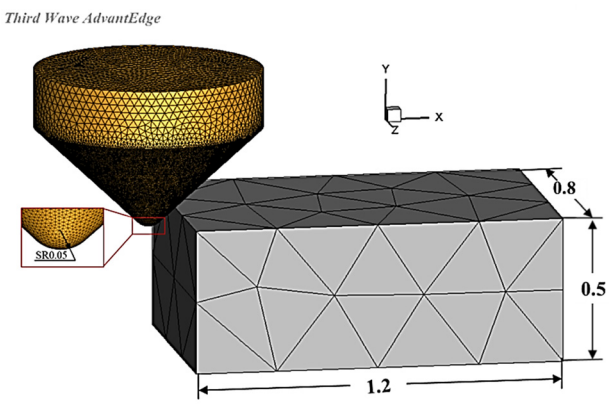

Fig. 5 The geometrical model

Table 1 The design of simulation

Simulation no.	1	2	3	4	5	6	7	8	9
Scratch depth (μm)	5	6	8	12	16	32	40	52	64

simplified comparing to that provided by Malkin when the ideal grit which is never worn during scratching process is applied to single grit scratch test. But the most serious problem is that such an ideal grit does not exist. Numerical simulation provides a solution to the problem, in which the wear can be defined as nonexistent.

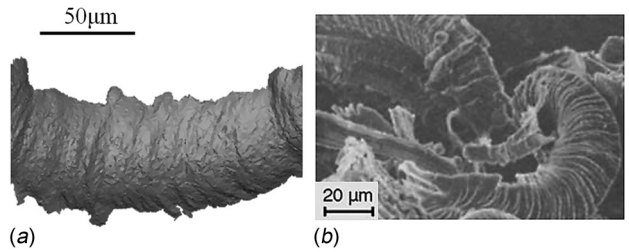

Fig. 7 The comparison of segmental chip: (*a*) the segmental chip acquired by simulation (scratching depth = 5 μm) and (*b*) the segmental chip presented by Malkin (scanning electron microscope) [3]

3 Numerical Simulation

3.1 The Process of Simulation. Single grit scratch simulation is performed with ADVANTEDGE (Third Wave Systems, Eden Prairie, MN), which integrates advanced finite element models for single grit scratch. The procedure of numerical calculation is shown in Fig. 2. Numerical simulation involves many models including material constitutive model, friction model, and thermal property model. The precision of the numerical simulation depends on the model whose accuracy is the worst.

3.2 The Physical Model. The Fe–Cr–Ni stainless steel and cubic boron nitride have been selected as the workpiece and grit material, respectively. Fe–Cr–Ni stainless steel is a commonly used material for steam turbine blades which is a kind of austenitic stainless steel. The steam turbine blades of Fe–Cr–Ni stainless steel usually formed using grinding process. The material model is the most important model in numerical simulation. Common material constitutive models include the Power–Law (P–L), the Johnson–Cook mode (J–C), and the Wright–Batra [17]. The material models including material constitutive and thermal property model of cubic Boron Nitride were offered by material library of ADVANTEDGE. The P–L constitutive model for workpiece material is used in the simulation, which considers strain strengthening, strain rate strengthening, and thermal softening. The material constitutive model of Fe–Cr–Ni stainless steel based on P–L relationship could be expressed as:

$$\sigma_s = \sigma_0\left(1+\frac{\varepsilon_s}{\varepsilon_0}\right)^{\frac{1}{n}} \times \left(1+\frac{\dot{\varepsilon}_s}{\dot{\varepsilon}_0}\right)^{\frac{1}{n}} \times \left(c_0 + c_1T + c_2T^2 + c_3T^3 + c_4T^4 + c_5T^5\right) \quad (9)$$

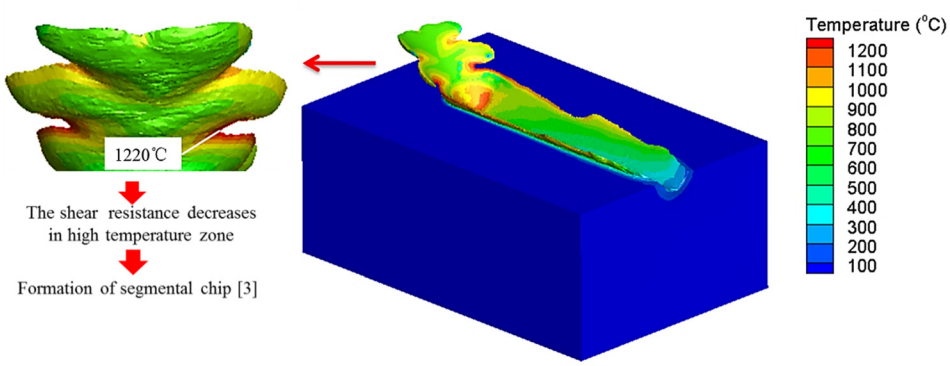

Fig. 6 Scratch morphology and temperature distribution (scratching depth = 40 μm)

Downloaded From: http://manufacturingscience.asmedigitalcollection.asme.org/ on 08/28/2018 Terms of Use: http://www.asme.org/about-asme/terms-of-use

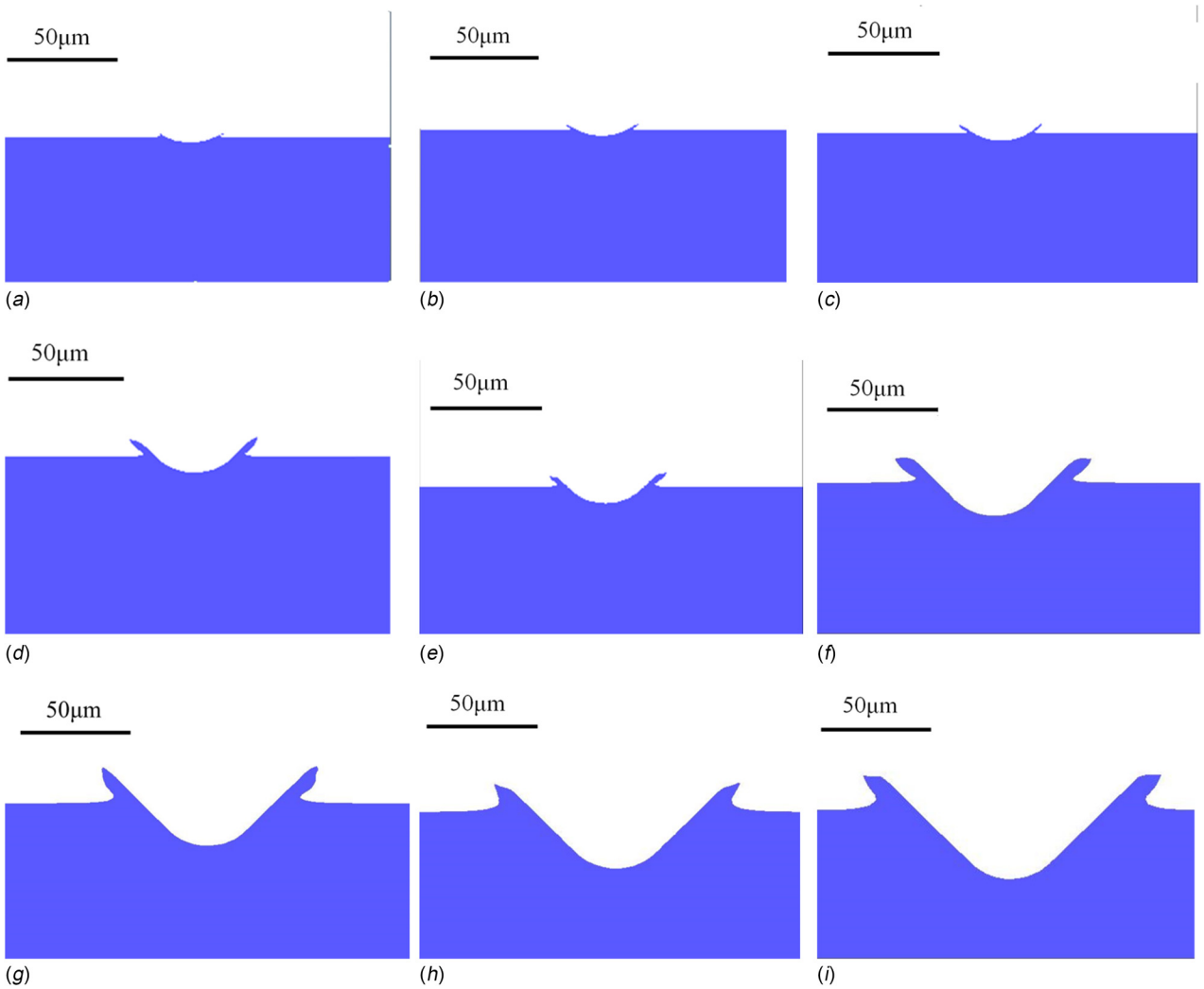

Fig. 8 Cross sections of scratches under different scratching depth: (*a*) scratching depth = 5 μm; (*b*) scratching depth = 6 μm; (*c*) scratching depth = 8 μm; (*d*) scratching depth = 12 μm; (*e*) scratching depth = 16 μm; (*f*) scratching depth = 32 μm; (*g*) scratching depth = 40 μm; (*h*) scratching depth = 52 μm; and (*i*) scratching depth = 64 μm

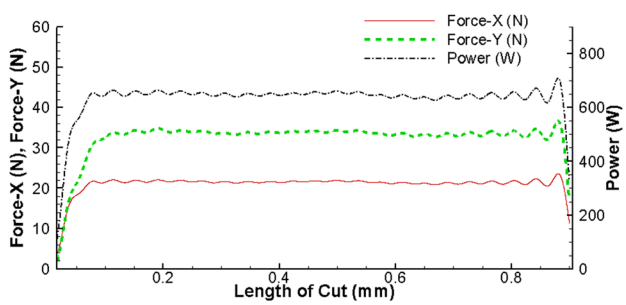

Fig. 9 Forces and power consumed by the scratching process (scratching depth = 40 μm)

where σ_s is the flow stress, and σ_0 is the yield stress at reference strain and temperature. T is the current deformation temperature, ε_0 is the reference strain, $\dot{\varepsilon}_o$ is the reference strain rate. m is strain-hardening exponent, n is the strain rate-hardening exponent, and $c_0 \sim c_5$ are material constants of constitutive model. The material constitutive model of Fe–Cr–Ni stainless steel has been developed by high temperature Hopkinson pressure bar technology, which is expressed as the following [18]:

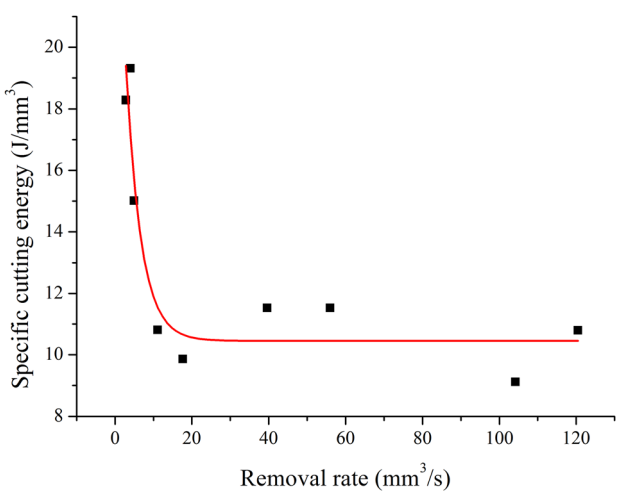

Fig. 10 Specific cutting energy versus material removal rate

Downloaded From: http://manufacturingscience.asmedigitalcollection.asme.org/ on 08/28/2018 Terms of Use: http://www.asme.org/about-asme/terms-of-use

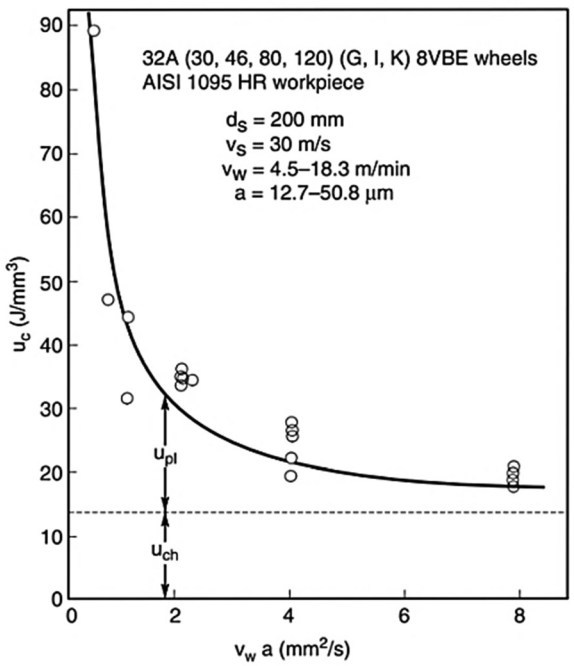

Fig. 11 Specific cutting energy versus material removal rate presented by Malkin [3]

$$\sigma_s = 1266.02\left(1+\frac{\varepsilon_s}{0.001}\right)^{\frac{1}{32.4465}} \times \left(1+\frac{\dot{\varepsilon}_s}{0.001}\right)^{\frac{1}{21.1104}} \times \left(1.0031 + 1.4784e^{-4}T - 5.7693e^{-6}T^2 + 1.9978e^{-8}T^3 - 3.0683e^{-11}T^4 + 1.6089e^{-14}T^5\right) \quad (10)$$

The proposed constitutive model has been incorporated in ADVANTEDGE to model orthogonal metal cutting process. Orthogonal turning tests with the same parameters as the simulation have been carried out in computer numerical control machine center. The comparison of test and simulation forces is shown in Fig. 3. The average error of the tangential force and normal force were 15.26% and 4.45%, respectively, which proves that the above material constitutive model has a high precision [18].

Thermal properties of Fe–Cr–Ni stainless steel including thermal conductivity and heat capacity have been measured by a laser flash diffusivity apparatus, and the measurement results are shown in Fig. 4 This material has a phase transition at 600–700 °C. The transition could cause the change of thermal physical properties. Using polynomial fitting method, the relationship of specific heat capacity and temperature has been fitted at 20–600 °C and 600–1000 °C, the result of the fitting are shown as following:

$$C_p = 0.3746 + 4.8492e^{-5}T + 6.1368e^{-7}T^2 \quad 20\,^\circ\mathrm{C} < T < 600\,^\circ\mathrm{C} \quad (11)$$

$$C_p = 2.6061 - 4.1607e^{-3}T + 1.9122e^{-6}T^2 \quad 600\,^\circ\mathrm{C} < T < 1000\,^\circ\mathrm{C} \quad (12)$$

Using polynomial fitting method, the relationship of thermal conductivity and temperature has been fitted at 20–500 °C and 500–1000 °C, the result of the fitting are shown as following:

$$K = 16.1603 + 2.7521e^{-2}T - 1.6998e^{-5}T^2 \quad 20\,^\circ\mathrm{C} < T < 500\,^\circ\mathrm{C} \quad (13)$$

$$K = 33.2295 - 1.7109e^{-2}T + 9.0011e^{-6}T^2 \quad 500\,^\circ\mathrm{C} < T < 1000\,^\circ\mathrm{C} \quad (14)$$

The ball on disk test has been carried out to determine the friction coefficient between grit and workpiece. The friction coefficient is defined as 0.25 according to the results, which has been inputted into ADVANTEDGE. The initial temperature is generally considered to be the room temperature, which was defned as 25 °C and inputted into ADVANTEDGE.

3.3 The Geometrical Model. The geometrical model is shown in Fig. 5. The computer-aided design model of the single grit has been developed and inputted into ADVANTEDGE which is a cone with the tip radius of 0.05 mm. The upper part of the cone is a cylinder for restricting the position of single grit on the simulation process. The grid at the tip of the cone is meshed very small to ensure the precision of the simulation, and the grid away from the tip is relatively large to improve the simulation efficiency. The workpiece is a cuboid, and the computer-aided design model can be defined directly in ADVANTEDGE by inputing the size parameters. The dimension of the workpiece is 1.2 mm × 0.8 mm × 0.5 mm, as shown in Fig. 5. The adaptive finite element mesh is the most important feature of the ADVANTEDGE. So the grid of the workpiece is not necessary to be meshed finely in the modeling process. The grid of workpiece closed to the grit is automatically refined appropriately, and the grid away from the grit is refined slightly during the simulation. The simulation precision and efficiency could be guaranteed due to the feature of ADVANTEDGE. The single grit is fixed, and the workpiece move relatively to the single grit with defined scratch depth. The related movement velocity and scratch depth could be inputted into ADVANTEDGE directly.

4 Design of Simulation

In the study of the relationship of specific energy and removal rate, the grinding speed should remain the same in order to eliminate the effect of grinding speed on the specific energy. The material removal rate of grinding depends on the feed rate of workpiece and the grinding depth when the grinding speed is constant. For a single grit scratch test, different material removal rates could be got directly by changing the scratching depth when the scratching speed is constant. A series of simulations have been designed with different scratching depths to acquire different removal rates. The scratching speed was 30 m/s for all group simulations. The design of simulation is shown in Table 1.

5 Results and Discussion

The simulation result of scratch morphology and temperature distribution is shown in Fig. 6. The material temperature of the contact area between the single grit and the workpiece is close to the melting point of the workpiece material. The phenomenon also exists in all group simulations which are listed in Table 1. The chip formation is extremely fast due to the high scratching speed. There is not enough time to pass the heat out, and single grit high speed scratching process can be considered an adiabatic process, which results in the temperature of the contact area is closed to the melting point. This viewpoint has been presented by Malkin and Guo [3]. Part of the material of workpiece flows toward the side of the grit to form the side flow and burr. At the same time, the segmental chip presented by Malkin is also found in the simulation results. The segmental chip acquired by simulation and that presented by Malkin are shown in Fig. 7. Malkin has presented the reason for the formation of segmental chip that is the shear resistance of the material decreases due to localized heated caused by intense plastic deformation [3]. As shown in Fig. 6, the temperature between the two lamellas is higher than that of the other parts, which confirms the viewpoint presented by Malkin.

The material removal volume of unit length of scratch could be acquired by comparison the cross section of workpiece defined in Sec. 3.3 before and after scratching, and the cross section of workpiece is shown in Fig. 8. The volume of material removed per unit

Downloaded From: http://manufacturingscience.asmedigitalcollection.asme.org/ on 08/28/2018 Terms of Use: http://www.asme.org/about-asme/terms-of-use

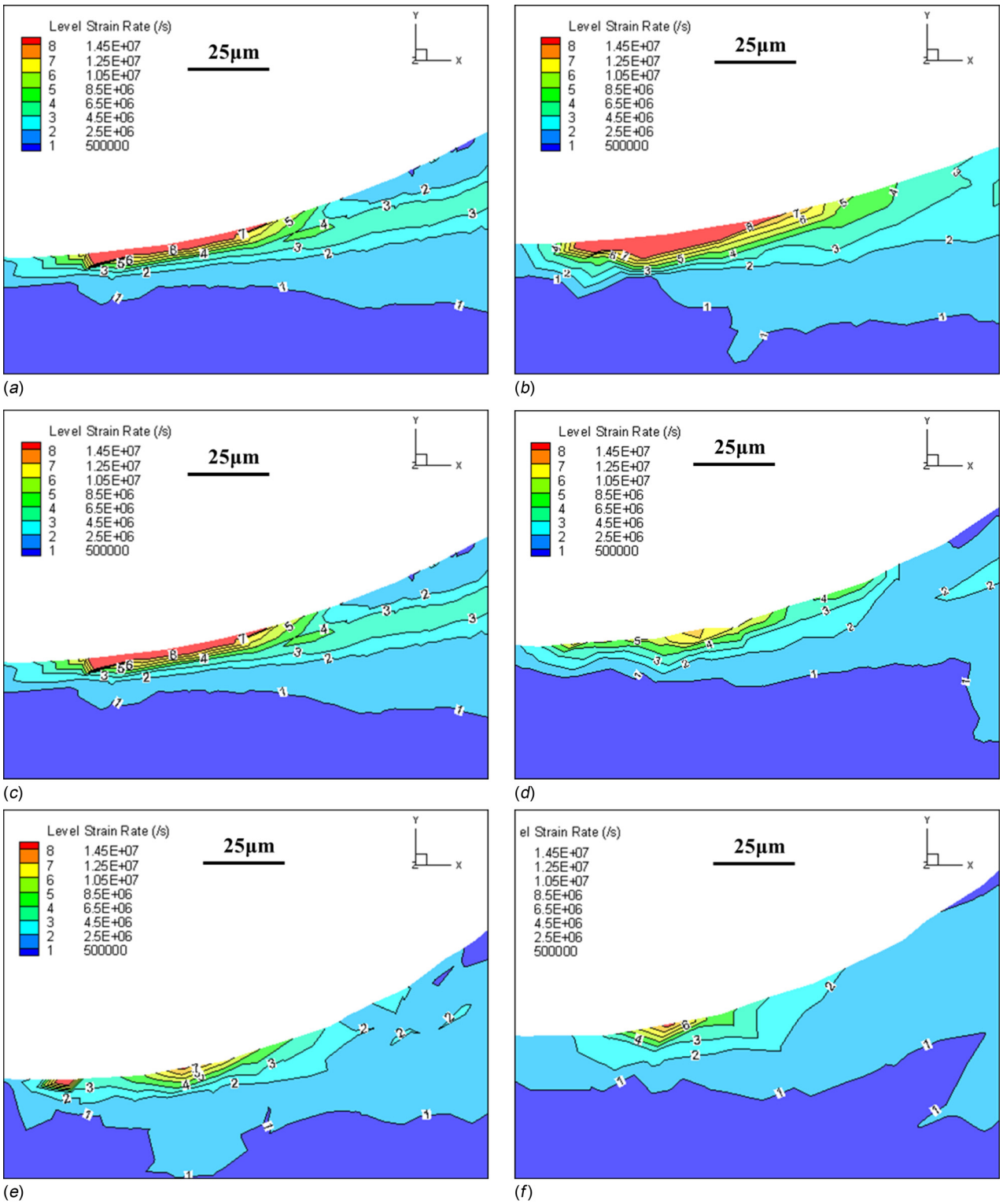

Fig. 12 The simulation results of strain rate (scratching velocity = 30 m/s): (*a*) scratching depth = 6 μm; (*b*) scratching depth = 8 μm; (*c*) scratching depth = 12 μm; (*d*) scratching depth = 16 μm; (*e*) scratching depth = 32 μm; (*f*) and scratching depth = 40 μm

time called removal rate could be calculated by combining the material removal volume of unit length of scratch and scratching speed. It is worth noting that the material removal rate is the actual material removal rate which considers that the side flow and burrs are not included in the material removal. Five material removal rates were calculated by intercepting five different cross sections for every scratch. The average of the five material removal rates is taken as the removal rate of the corresponding scratch process. ADVANTEDGE can record the forces applied on grit and the power consumed by the scratching process timely as

Downloaded From: http://manufacturingscience.asmedigitalcollection.asme.org/ on 08/28/2018 Terms of Use: http://www.asme.org/about-asme/terms-of-use

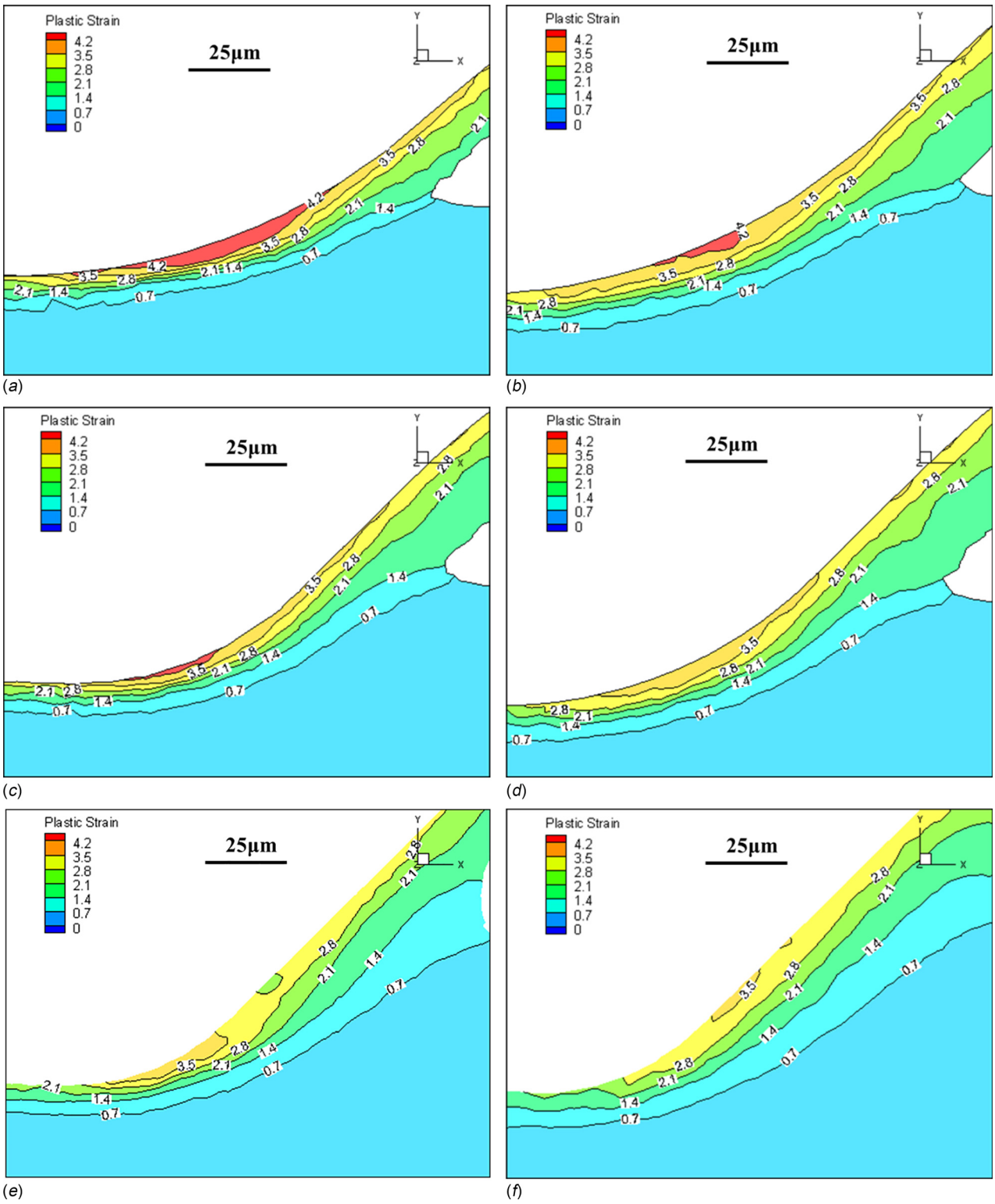

Fig. 13 The simulation results of plastic strain (sScratching velocity = 30 m/s): (*a*) scratching depth = 6 μm; (*b*) scratching depth = 8 μm; (*c*) scratching depth = 12 μm; (*d*) scratching depth = 16 μm; (*e*) scratching depth = 32 μm; and (*f*) scratching depth = 40 μm

shown in Fig. 9. The forces and power curves are smooth, which shows the stability of simulation. Then, the specific cutting energy can be calculated by the following equation:

$$u_c = \frac{P}{Q_w} \tag{15}$$

where u_c (J/mm^3) is the specific cutting energy; P (W) is the power consumed of scratching process; Q_w is the removal rate (mm^3/s).

The specific cutting energy under different material removal rates is shown in Fig. 10. It is shown that the specific cutting energy increases drastically with the decrease of removal rate.

Downloaded From: http://manufacturingscience.asmedigitalcollection.asme.org/ on 08/28/2018 Terms of Use: http://www.asme.org/about-asme/terms-of-use

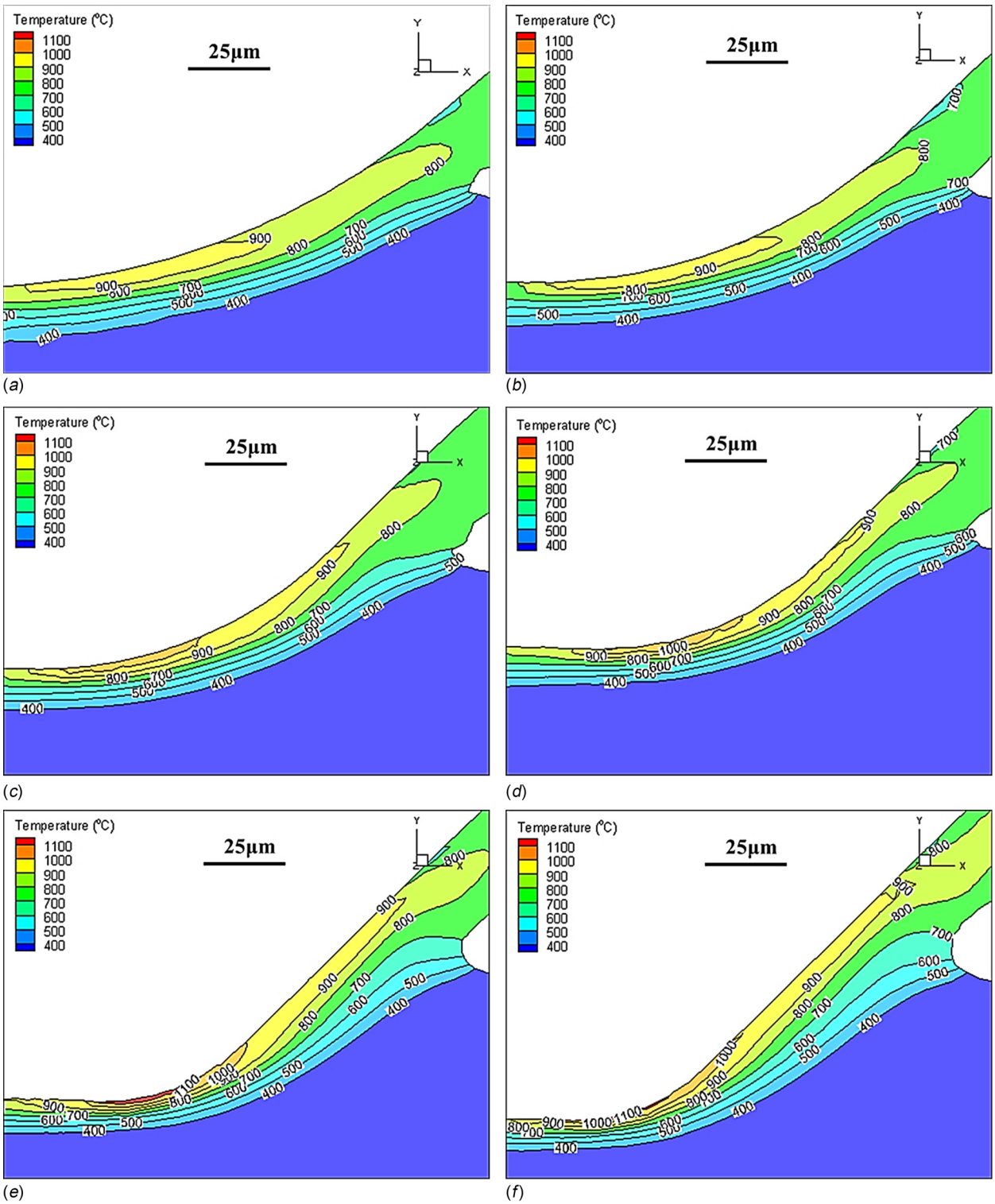

Fig. 14 The simulation results of temperature (scratching velocity = 30 m/s): (*a*) scratching depth = 6 μm; (*b*) scratching depth = 8 μm; (*c*) scratching depth = 12 μm; (*d*) scratching depth = 16 μm; (*e*) scratching depth = 32 μm; and (*f*) scratching depth = 40 μm

Malkin has also presented the change trend of specific cutting energy with the variety of material removal rate as shown in Fig. 11. The simulation results agree well with Fig. 11. It is worth noting that the simulation cannot be carried out when the cutting depth is extremely small due to the limitation of ADVANTEDGE itself. The simulations just give the specific cutting energy when the material removal rate is large. However, the simulation results have shown the trend of specific cutting energy with the change of material removal rate clearly.

The strain rate, plastic strain, and temperature of the workpiece material have been analyzed for several groups simulations with different scratching depths because of its representation. In order to acquire comprehensive results, scratches for different scratching depths are cut along the centerline. The results of strain rate,

Downloaded From: http://manufacturingscience.asmedigitalcollection.asme.org/ on 08/28/2018 Terms of Use: http://www.asme.org/about-asme/terms-of-use

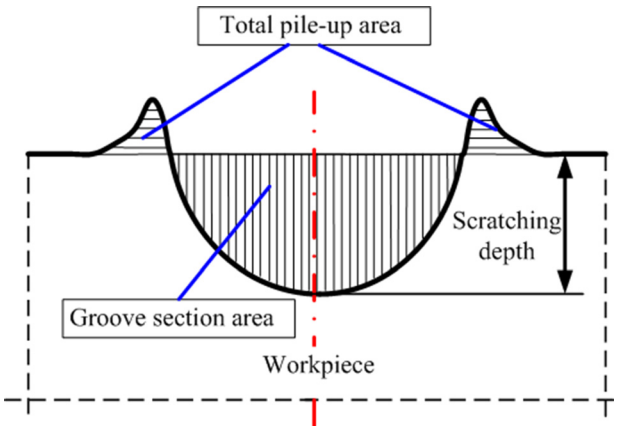

Fig. 15 Cross section profile of scratch

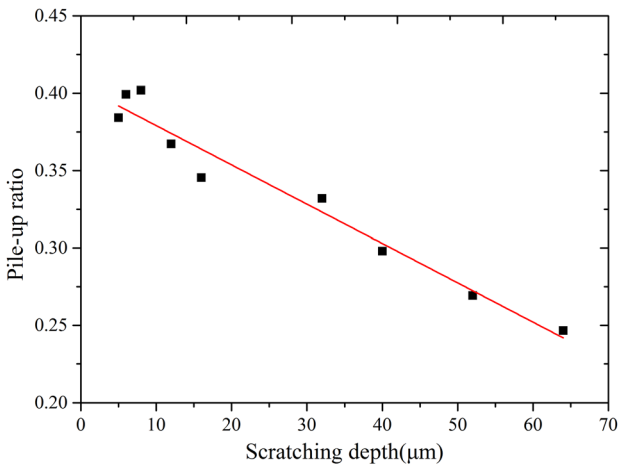

Fig. 16 Pile-up ratio versus scratching depth

plastic strain, and temperature of the workpiece are shown in Figs. 12–14, respectively. It is found that the strain rate increases with the decrease of scratching depth due to the decrease of shear angle caused by the increase of average negative rake angle, and the increase of average negative rake angle is due to the blunt round at the tip of grit. It is also found that the plastic strain increases with the decrease of scratching depth, and the material temperature decreases with the decrease of the scratching depth. The strain rate, plastic strain, and temperature together determine the flow stress of workpiece material according to Eq. (9). So the material flow stress increases with the decrease of scratching depth that is material removal rate according to the above analysis. It means that more energy is consumed during the scratching process due to the increase of the flow stress when the scratching depth is small, which caused the size effect of specific cutting energy.

Material removal mechanisms of different scratching depth have different characteristics in terms of ploughing and cutting. Prominent action will be determined by using the measure of pile up ratio as shown in Fig. 15, and the pile-up ratio is defined as the total pile-up area divided by groove section area, which is expressed as following equation:

$$\rho = \frac{A_P}{A_G}$$

where ρ is the pile-up ratio, A_P is the total pile-up area, and A_G is the groove section area. The pile-up ratio for different scratching ratio is shown in Fig. 16. It is found that the pile-up ratio decreases almost linearly with the increase of scratching depth, which could explain the size effect of specific cutting energy from another perspective.

6 Conclusions

- A method of research on the size effect of the specific cutting energy based on the numerical simulation has been proposed. The theoretical model of the research on size effect of specific cutting energy using single grit scratching simulation was presented.
- A series of single grit scratching simulations with different scratching depths have been carried out, and the specific cutting energy was calculated based on the power consumed and the material removal rate. The relationship between the specific cutting energy and the material removal rate has been given which agrees well with that presented by Malkin.
- The conclusion has been got that the flow stress increases with the decrease of removal rate, which explains the relationship between specific cutting energy and material removal rate well.
- The pile-up ratio decreases almost linearly with the increase of scratching depth, which could explain the size effect of specific cutting energy from another perspective.

Funding Data

- National Natural Science Foundation of China (51475173).
- Natural Science Foundation of Fujian Province (2016J01237).

References

[1] Shaw, M., 1974, "The Size Effect in Metal Cutting," Sadhana, **28**(5), pp. 875–896.
[2] Malkin, S., 1975, "Minimum Energy in Abrasive Processes," WEAR, **32**(1), pp. 15–23.
[3] Malkin, S., and Guo, C., 2008, *Grinding Technology-Theory and Application of Machining With Abrasives*, 2nd ed., Indusry press, New York.
[4] Kannapan, S., and Malkin, S., 1972, "Effects of Grain Size and Operating Parameters on the Mechanics of Grinding," ASME J. Eng. Ind., **94**(3), pp. 833–842.
[5] Malkin, S., and Murray, T., 1977, "Comparison of Single Point and Rotary Dressing of Grinding Wheels," Fifth North American Metalworking Research Conference, Amherst, MA, May 23–25, p. 278.
[6] Malkin, S., 1975, "Specific Energy and Mechanisms in Abrasive Processes," Third North American Metalworking Research Conference, pp. 453–465.
[7] Chen, X., and Tecelli, T., 2013, "Comparison of Material Removal Characteristics in Single and Multiple Cutting Edge Scratches," Adv. Mater. Res., **179**, pp. 189–195.
[8] Von Turkovich, B. F., 1970, "Shear Stress in Metal Cutting," ASME J. Eng. Ind., **92**(1), pp. 151–157.
[9] Bomin, L., and Bo, Z., 2003, *Modern Grinding Technology*, Machinery Industry Press.
[10] Rowe, W. B., and Chen, X., 2010, "Characterization of the Size Effect in Grinding and the Sliced Bread Analogy," Int. J. Prod. Res., **35**(3), pp. 887–899.
[11] Ren, Y. H., Zhang, B., and Zhou, Z. X., 2009, "Specific Energy in Grinding of Tungsten Carbides of Various Grain Sizes," CIRP Ann. Manuf. Technol., **58**(1), pp. 299–302.
[12] Brinksmeler, E., and Glwerzew, A., 2003, "Chip Formation Mechanisms in Grinding at Low Speeds," CIRP Ann. Manuf. Technol., **52**(1), pp. 253–258.
[13] Wang, H., Subhash, G., and Chandra, A., 2001, "Characteristics of Single-Grit Rotating Scratch With a Conical Tool on Pure Titanium," WEAR, **249**(7), pp. 566–581.
[14] Zhu, D., Yan, S., and Li, B., 2014, "Single-Grit Modeling and Simulation of Crack Initiation and Propagation in SiC Grinding Using Maximum Undeformed Chip Thickness," Comput. Mater. Sci., **92**, pp. 13–21.
[15] Duan, N., Yu, Y., Wang, W., and Xu, X., 2016, "SPH and FE Coupled 3D Simulation of Monocrystal SiC Scratching by Single Diamond Grit," Int. J. Refractory Met. Hard Mater., **64**, pp. 279–293.
[16] Pen, H. M., Liang, Y. C., Luo, X. C., Bai, Q. S., and Goel, S., 2011, "Multiscale Simulation of Nanometric Cutting of Single Crystal Copper and Its Experimental Validation," Comput. Mater. Sci., **50**(2), pp. 3431–3441.
[17] Zhang, T., Jiang, F., Yan, L., and Xu, X., 2017, "Research on the Stress and Material Flow With Single Particle—Simulations and Experiments," J. Mater. Eng. Perform., **26**(6), pp. 2689–2697.
[18] Yu, J., Jiang, F., Rong, Y., Xie, H., and Suo, T., 2014, "Numerical Study the Flow Stress in the Machining Process," Int. J. Adv. Manuf. Technol., **74**(1–4), pp. 509–517.

Downloaded From: http://manufacturingscience.asmedigitalcollection.asme.org/ on 08/28/2018 Terms of Use: http://www.asme.org/about-asme/terms-of-use